Journal of Power Sources 243 (2013) 796–804

Contents lists available at SciVerse ScienceDirect

Journal of Power Sources

journal homepage: www.elsevier.com/locate/jpowsour

Synthesis and properties of phenylindane-containing polybenzimidazole (PBI) for high-temperature polymer electrolyte membrane fuel cells (PEMFCs)

Xin Li [a], Xiaoming Chen [b], Brian C. Benicewicz [a,*]

[a] Department of Chemistry and Biochemistry, University of South Carolina, Columbia, SC 29208, USA
[b] Department of Chemical Engineering, University of South Carolina, Columbia, SC 29208, USA

HIGHLIGHTS

- A novel phenylindane-containing PBI was synthesized in PPA for the first time.
- Polymer solubility greatly improved by incorporating rigid bent phenylindane moiety.
- Phenylindane-PBI showed comparable thermal and mechanical stability as *meta*-PBI.
- A peak power density of 360 mW cm^{-2} was achieved at 180 °C under H_2/air without external humidification.

ARTICLE INFO

Article history:
Received 11 March 2013
Received in revised form
9 May 2013
Accepted 7 June 2013
Available online 14 June 2013

Keywords:
Fuel cell
High temperature
Polymer electrolyte membrane
Polybenzimidazole
Phosphoric acid
Phenylindane

ABSTRACT

A thermally stable and organo-soluble phenylindane-containing polybenzimidazole (phenylindane-PBI) was synthesized from 3,3′,4,4′-tetraaminobiphenyl and 1,1,3-trimethyl-3-phenylindan-4′,5-dicarboxylic acid using polyphosphoric acid (PPA) as both solvent and dehydrating agent. Polymerization conditions were carefully investigated to achieve high molecular weight polymers (IV = 1.00 dL g^{-1}). To study the effects of backbone structure on properties, *meta*-PBI was also synthesized in PPA. It was found the introduction of rigid bent phenylindane moiety into the polymer backbone greatly improved the polymer solubility in polar aprotic solvents. The fabrication of acid-doped phenylindane-PBI membranes was attempted by both sol–gel and acid imbibing processes. The membranes prepared by the latter method showed a maximum proton conductivity of 0.061 S cm^{-1} at 180 °C with a phosphoric acid doping level of 10.0 PA/RU. Both phenylindane-PBI and *meta*-PBI membranes were fabricated into membrane electrode assemblies (MEAs) and tested to evaluate their fuel cell performance. The phosphoric acid doped phenylindane-PBI membrane exhibited comparable fuel cell performance as *meta*-PBI under similar testing conditions, demonstrating that it is a promising polymer electrolyte membrane candidate for high-temperature fuel cell applications.

© 2013 Elsevier B.V. All rights reserved.

1. Introduction

In recent years, high-temperature proton exchange membrane fuel cells (PEMFCs) operating at 120–200 °C have been considered as very promising candidates for both transportation and stationary applications. Compared with traditional low temperature PEMFC systems (operated < 100 °C), they may provide several benefits such as improved catalyst kinetics, higher tolerance to fuel impurities (e.g. CO), simplified reformation schemes, and increased efficiency for the cogeneration of heat and electricity [1–5]. As the key part of the PEMFC, the polymer electrolyte membrane (PEM) plays an important role in deciding the device's final performance and reliability. Among various types of novel PEM materials that have been developed so far, the polybenzimidazole (PBI)–phosphoric acid (PA) complex membrane system is considered as the most effective one to meet requirements such as high proton conductivity and good chemical and thermal stability for high-temperature operations.

Although PBI represents a large family of heterocyclic polymers containing the benzimidazole moiety as part of the polymer repeat unit, many people use the acronym for one specific PBI variant – poly[2,2′-(*m*-phenylene)-5,5′-bibenzimidazole] (*meta*-PBI), since it is the only commercialized PBI product originally produced by Celanese Corp. (now by PBI Performance Products). In 1995,

* Corresponding author. Tel.: +1 (803) 777 0778; fax: +1 (803) 777 8100.
E-mail address: benice@sc.edu (B.C. Benicewicz).

0378-7753/$ – see front matter © 2013 Elsevier B.V. All rights reserved.
http://dx.doi.org/10.1016/j.jpowsour.2013.06.033

Wainright et al. first described the idea that PBI could be doped with low vapor pressure inorganic proton conductors such as PA to use in high-temperature fuel cells [6]. Since then, tremendous work has been done on modifying the PEM systems based on *meta*-PBI via different approaches. The typical strategies include optimization of membrane fabrication techniques [7–10], polymer cross-linking [11–14], polymer blend membranes [15–18], polymer composite membranes [19,20], etc. However, the improvements have been relatively limited and the PBI systems still suffer from drawbacks such as weak mechanical strength at high acid loading and poor long-term stability. Another issue with *meta*-PBI is its poor processability. The polymer chains of *meta*-PBI are closely correlated due to the intermolecular hydrogen bonding and π–π stacking, thus the polymer has a high T_g (~425 °C) and can only dissolve in a few polar aprotic solvents such as *N*,*N*-dimethylacetamide (DMAc) and *N*-methylpyrrolidone (NMP) at relatively low concentrations.

Instead of relying solely on the chemical and physical modifications of *meta*-PBI, investigations of new PBI chemical structures at the molecular level provides us a much broader window to study and design this class of materials to potentially achieve better combinations of properties. One advantage of PBI synthesis is that the chemistry is relatively straightforward. To synthesize PBIs at the laboratory-scale usually only requires a single-step solution polycondensation reaction from tetraamines and dicarboxylic acids or their simple derivatives. By varying the structure of the monomers, especially the structure of dicarboxylic acid, it is easy to alter the PBI backbone, morphology and several other corresponding properties, which would enhance our understanding of the structure–property relationships within these materials. Surprisingly, there is only limited research on new PBI structures with the detailed study of their corresponding fuel cell properties. These include PBIs containing partially fluorinated groups [21,22], sulfone linkages [18,23], and ether linkages [24]. By using a novel sol–gel process, we have successfully synthesized a series of novel PBIs with higher acid doping levels and improved properties [10,25–27]. These results also confirmed that the chemical structure of PBIs affects the final fuel cell performance, thus supporting the view that efforts are needed to fully understand structure–property relationships.

Among numerous potential functional moieties that could be examined to improve the processability of PBI polymers, the phenylindane group has not been previously considered. First, there are very limited reports about PBIs containing aliphatic groups, especially with a full study of their physicochemical properties as potential PEM materials [28,29]. Bhavsar et al. synthesized a series of PBIs containing linear aliphatic moieties with increasing number of $-CH_2-$ groups and found the membranes prepared by the sol–gel process showed high acid loading (up to 32 PA/RU) and several other comparable properties as those of fully aromatic PBIs [29]. Therefore, it would be interesting to introduce an aliphatic ring moiety into the PBI backbone that could help further understand the structure–property relationship of PBIs. Second, the phenylindane group possesses a rigid and bent structure, which could potentially disrupt the chain packing and improve the polymer solubility when introduced into the PBI backbone [30–32]. As an example, Ding et al. synthesized a series of novel polyamides containing the phenylindane moieties which exhibited good solubility in polar organic solvents and several other improved properties [30]. Another example is the commercially available polyimide, Matrimid®, which is highly soluble in common organic solvents such as methylene chloride and tetrahydrofuran, exhibits a high T_g (dry film, 265 °C) and good gas transport properties. Also, the PBI morphology changes caused by the introduction of the phenylindane functionality are expected to affect several corresponding polymer properties as PEM materials, such as water uptake, acid swelling ability, proton conductivity, and mechanical strength.

In this work, we have successfully prepared a PBI variant containing the phenylindane moiety (phenylindane-PBI) as well as the highly studied *meta*-PBI by solution polymerization in polyphosphoric acid (PPA) for detailed comparisons. The polymerization conditions of phenylindane-PBI were carefully studied to obtain high molecular weight polymers. The introduction of the new functional group improved the polymer's solubility while still maintaining good thermal stability as compared to *meta*-PBI. Both PBIs were fabricated into membranes using both of the major membrane fabrication processes and their corresponding properties such as acid doping behavior, mechanical stability and proton conductivity were compared. The phenylindane-PBI exhibited some improved properties as compared to *meta*-PBI, indicating it is promising candidate for novel PEM materials.

2. Experimental

2.1. Materials

3,3′,4,4′-Tetraaminobiphenyl (TAB, polymer grade, ~97.5%) was donated by BASF Fuel Cell. 1,1,3-Trimethyl-3-phenylindan-4′,5-dicarboxylic acid (phenylindane diacid) and isophthalic acid (IPA) were purchased from Amoco Chemicals. Polyphosphoric acid (PPA, 115%) was purchased from Aldrich Chemical. Phosphoric acid (PA, 85%) was purchased from Fisher Scientific. All the other common solvents such as *N*,*N*-dimethylacetamide (DMAc), *N*-methylpyrrolidone (NMP), and *N*,*N*-dimethylformamide (DMF) were purchased from Fisher Scientific. Unless otherwise specified, all chemicals were used as received.

2.2. Polymer synthesis

In a typical synthetic procedure for phenylindane-PBI, TAB (2.143 g, 10 mmol), phenylindane diacid (3.243 g, 10 mmol), and PPA (60–100 g) were added to a 100 ml round-bottomed flask equipped with an overhead mechanical stirrer and nitrogen inlet/outlet. The reaction solution was mechanically stirred at 50 rpm and purged with slow nitrogen flow during the entire reaction. A programmable temperature controller with ramp and soak features was used to control the reaction temperatures. The following general temperature profile was used: stir at 50 °C for 1 h, ramp to 140 °C over 2 h, stir at 140 °C for 4 h, ramp to 175 °C over 3 h, stir at 175 °C for 6 h, ramp to 195 °C over 2 h, stir at 195 °C for 35 h. As the polymerization proceeded, the solution developed a dark brown color and became more viscous. Then the polymer solution was poured into water to quench the reaction, pulverized, neutralized with ammonium hydroxide, and dried in oven at 110 °C overnight to obtain the products. The synthetic procedure of *meta*-PBI was similar and the detailed reaction conditions (e.g. monomer charge, temperature, time) were described previously [33].

2.3. PBI membrane preparation

2.3.1. PPA process

At the end of polymerization, the hot phenylindane-PBI/PPA solution (approximately 60–80 g) was poured onto a clean flat glass substrate (size: 35 cm × 25 cm; preheated in oven at 130 °C) and then cast in air using a film applicator with gate thicknesses varying from 15 mils (0.381 mm) to 25 mils (0.635 mm). The whole plate was then transferred to a humidity chamber with relative humidity of 55% for 24 h to obtain the PA-doped PBI membrane. Further preparation details can also be found in previously published work [10,27].

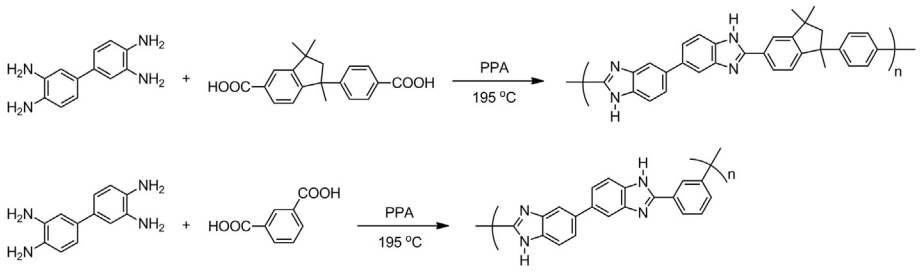

Fig. 1. Synthesis of phenylindane-PBI (upper) and *meta*-PBI (lower) in PPA.

2.3.2. Conventional PA imbibing process

The general membrane preparation procedure for both phenylindane-PBI and *meta*-PBI was described herein: 1.000 g PBI powder was mixed with approximately 30 ml DMAc in a 100 ml round-bottom flask and then refluxed for 3–4 h until most polymers were dissolved. After the solution was cooled to r.t., centrifugation at 6000 rpm for 30 min was applied to remove the undissolved or swollen parts. PBI dense membrane was then cast in a glove bag under dry nitrogen atmosphere. The PBI solution was poured onto a clean glass plate which was taped with glass slides on each side to restrain the movement of the solution. After casting, the membrane was pre-dried inside the glove bag with a hotplate temperature of 40–50 °C overnight to remove most solvent. Then the film was transferred to the vacuum oven and dried at 110 °C overnight to obtain the PBI dense membrane. The acid-doped membrane was prepared by soaking the PBI dense membrane into different concentration PA solutions for more than 48 h.

2.4. Characterization techniques

2.4.1. Polymer characterization

^{1}H NMR spectra were recorded on a Varian Mercury 400 spectrometer. FTIR spectra were recorded on a PerkinElmer Spectrum 100 FT-IR spectrometer with a three reflection diamond/ZnSe crystal. The inherent viscosities (IV's) of the polymers were measured with a Cannon Ubbelohde viscometer at a polymer concentration of 0.2 g dL^{-1} in concentrated sulfuric acid (96 wt%) at 30 °C. Thermogravimetric analysis (TGA) thermograms were obtained using TA Q5000 IR Thermogravimetric Analyzer at a heating rate of 10 °C min^{-1} under nitrogen flow (20 ml min^{-1}). The densities of polymers were measured with a Kimble* Kimax* specific gravity bottle using cyclohexane as solvent at 30 °C. The solubility of PBIs was evaluated by mixing PBIs with respective solvents and shaking on a wrist action shaker at r.t. for approximately 48 h.

2.4.2. Membrane characterization

The tensile properties of the PBI membranes were measured by TA RSA III Solid Analyzer at a constant Hencky strain rate of 0.001 s^{-1} at ambient condition without environment control. PBI specimens were cut according to ASTM D882 standard. The PA doping level, expressed as moles of PA per mole of PBI repeat unit (PA/RU), was measured using a Metrohm 716 DMS Titrino Automated Titrator with 0.01 M NaOH solution and calculated according to Eq. (1). The V_{NaOH} and C_{NaOH} are the volume and concentration of the NaOH required for the neutralization to reach the first equivalent point (EP1). The M_w is the molecular weight of the PBI repeat unit. The W_{dry} is the dry weight of the polymer obtaining by heating the sample in oven at 110 °C overnight after titration. Through-plane proton conductivities (σ) of PBI membranes were measured by a four-probe AC impedance method using a Zahner IM6e electrochemical station with a frequency range from 1 Hz to 100 kHz and amplitude of 5 mV. According to Eq. (2), the D is the distance between two inner electrodes. The W and T are the width and thickness of the membrane. R is the experimental value of membrane impedance. During the testing, a programmable oven was used to control the testing temperatures following an initial heating cycle from r.t. to 180 °C to remove the water from the membrane. The detailed measurement method and fitting model was described previously [10].

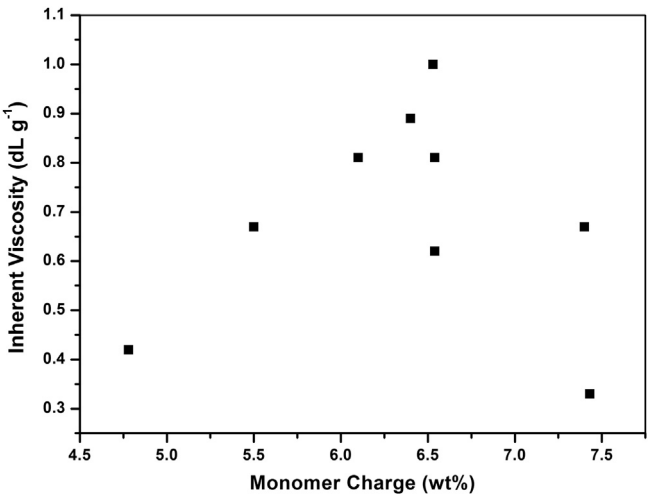

Fig. 2. Effect of monomer concentration on IV for phenylindane-PBI at a polymerization temperature of 195 °C.

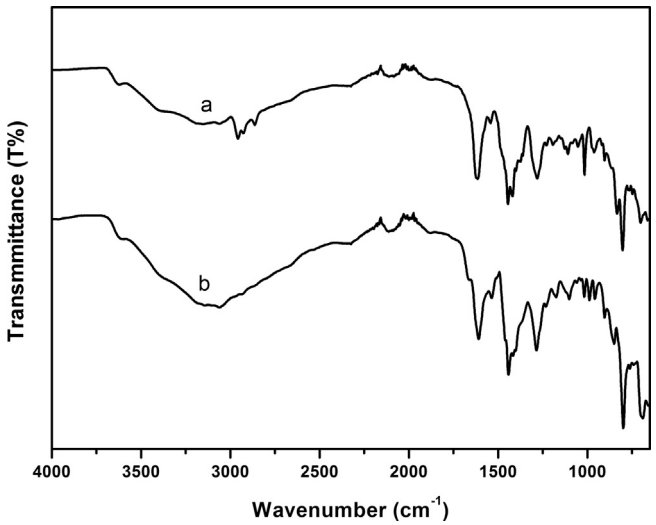

Fig. 3. FTIR spectrum of phenylindane-PBI (a) and *meta*-PBI (b).

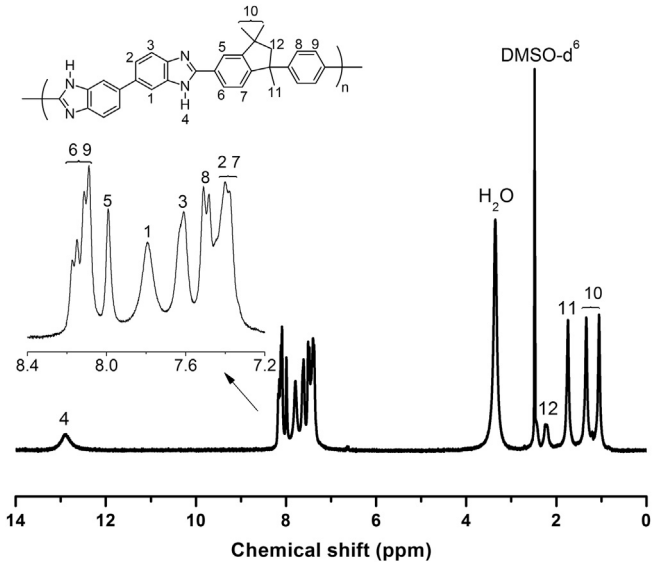

Fig. 4. ^{1}H NMR spectrum of phenylindane-PBI.

$$X = (V_{NaOH} \times C_{NaOH} \times M_w)/W_{dry} \quad (1)$$

$$\sigma = D/(W \times T \times R) \quad (2)$$

2.5. Membrane electrode assembly (MEA) fabrication and fuel cell testing

Single cells with active area of 10.15 cm^2 were used to measure the fuel cell performance of the PBI membranes. The gas diffusion electrodes (GDE) were acquired from BASF Fuel Cell and the catalyst loading on anode and cathode sides were 1.0 mg cm^{-2} Pt and 1.0 mg cm^{-2} Pt alloy, respectively. To fabricate the MEA, the membrane was quickly dipped into 85% PA solution for 10–20 s, placed between the anode and cathode electrodes, and then hot-pressed at 140 °C and 6 N cm^{-2} for 600 s. The MEA was then assembled into a single cell fuel cell testing hardware. The fuel cell fabrication consisted of following components (from anode side to the MEA): stainless steel end plate with attached heater, anode current collector, gas flow field plate, and MEA. After assembly, the bolts of the cell were tightened evenly with 45 in-lbs torque. Fuel cell performance testing was conducted using a commercial fuel cell testing station from Fuel Cell Technology. All the gases (fuel and oxidant gases) were used without humidification and fed to the anode and cathode at a stoichiometric ratio of 1.2 and 2.0, respectively, in flow tracking mode.

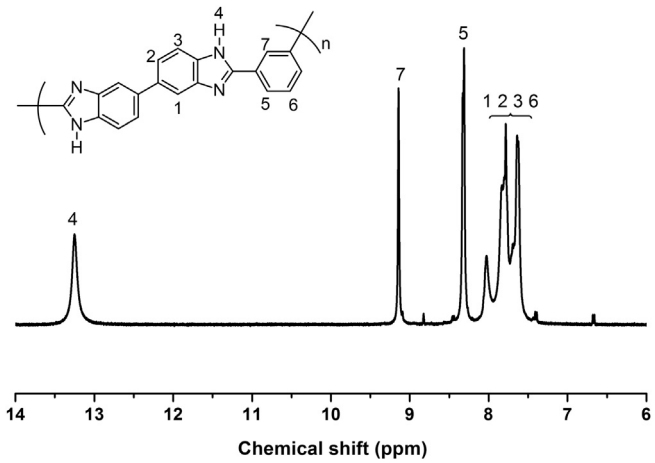

Fig. 5. ^{1}H NMR spectra of *meta*-PBI.

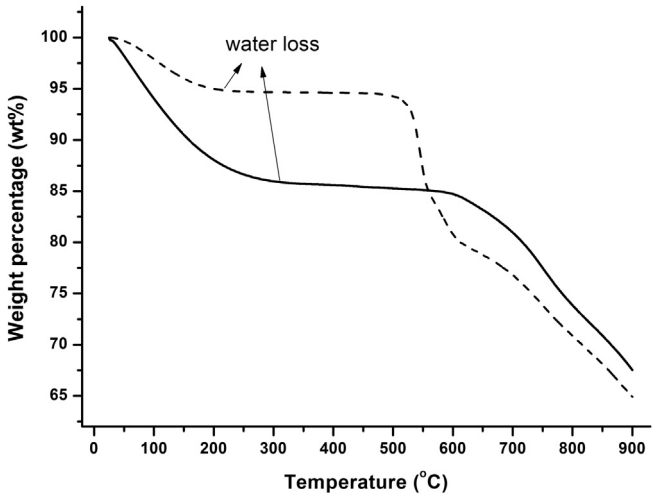

Fig. 6. TGA thermograms of phenylindane (solid) and *meta*-PBI (dash) under nitrogen atmosphere.

3. Results and discussion

3.1. Polymer synthesis and characterization

3.1.1. Polymer synthesis

Synthetic approaches for PBI polymers have been studied for several decades and two common methods are the melt/solid polymerization and solution polymerization. A two-stage melt/solid polymerization has been applied to the production of commercial *meta*-PBI and has some advantages for industrial production such as solvent-less conditions and easy processing after the reaction. However, the IV's of the *meta*-PBI are relatively limited due to the characteristics of the heterogeneous reaction conditions. A few patents reported the synthesis of phenylindane-PBI by the two-stage melt/solid polymerization and polymers with IV's as high as 0.63 dL g^{-1} (measured at a concentration of 0.4 wt% in concentrated sulfuric acid (97 wt%)) were produced [34–36]. However, the solution polymerization of PBIs in PPA is more convenient for laboratory study since it uses milder reaction temperatures and homogeneous reaction conditions, and can easily produce high molecular weight polymers. Therefore, the synthesis of phenylindane-PBI from TAB and phenylindane diacid by solution polymerization in PPA was investigated in this study (Fig. 1).

Table 1
Physical properties of PBI variants.

Polymer	Density (g cm^{-3})	Estimated FFV[a]	TGA				
			Water loss (wt%)[b]	$TD_{0.02}$ (°C)[c]	TD_5 (°C)[c]	TD_{10} (°C)[c]	T900 (wt%)[d]
Phenylindane-PBI	1.16	0.162	5.56	315.9	541.9	558.0	68.54
meta-PBI	1.33	0.136	16.73	379.4	691.2	753.7	78.8

[a] Fractional free volume (FFV) was calculated from Bondi's group contribution approach [40].
[b] Water content from the initial weight loss.
[c] Temperature at which 0.02%, 5%, and 10% weight loss occurred, respectively.
[d] Retained weight% at 900 °C.

Table 2
Solubility characteristics of phenylindane-PBI and *meta*-PBI.

Polymer	IV (dL g^{-1})	DMAc	LiCl/DMAc	NMP	DMF	Acetone	THF	MeOH
Phenylindane-PBI	1	++	++	++	++	−	−	−
meta-PBI	1.39	+	+	+	+	−	−	−

DMAc: *N*,*N*-dimethylacetamide; LiCl/DMAc: 4 wt% LiCl in DMAc; NMP: *N*-methyl-2-pyrrolidinone; DMF: dimethylformamide; THF: tetrahydrofuran; MeOH: methanol. ++: mostly soluble with 10.0 wt% PBI solution; +: partially soluble with polymer swelling with 3.0 wt% PBI solution; −: insoluble.

Polymerization conditions for the phenylindane-PBI were experimentally determined and Fig. 2 shows the results for polymerization conducted at 195 °C with varying monomer concentrations. Under these conditions, a maximum IV (IV = 1.00 dL g^{-1}) was observed for monomer concentrations of approximately 6.5 wt%. The step growth reaction was inhibited when the monomer concentration was too low and only low IV polymers were obtained (dilution effect). When the monomer concentration was higher than 6.5 wt%, the polymer solution became too viscous for efficient stirring, which also resulted in lower polymer molecular weight. For comparison, *meta*-PBI was also prepared in PPA (Fig. 1) following literature protocols and relatively high molecular weight polymers (IV = 1.18–1.39 dL g^{-1}) were produced [33].

3.1.2. Spectral characterization

The FTIR spectra of both phenylindane-PBI and *meta*-PBI are shown in Fig. 3 and exhibited common absorptions at 3150 cm^{-1}, 1600 cm^{-1}, 1430 cm^{-1} and 1410 cm^{-1}. The band at 3150 cm^{-1} corresponds to the stretching vibration of the hydrogen bonded N–H group. The region 1650–1400 cm^{-1} is characteristic of the benzimidazole ring and these bands were mostly attributed to the C=C and C=N stretching and the benzimidazole ring vibration. For phenylindane-PBI, absorption peaks at 2859–2960 cm^{-1} were observed, which were attributed to the aliphatic C–H bonds in the aliphatic ring of the phenylindane moiety. Both PBIs were also characterized by ^{1}H NMR using DMSO-d_6 solvent as shown in Figs. 4 and 5. The characteristic proton signals of benzimidazole unit were observed, such as the imidazole protons (H_4; 12.7–13.5 ppm) and biphenyl protons (H_1, H_2, and H_3; 7.5–8.2 ppm). These characterizations confirmed the successful preparation of desired phenylindane-PBI and *meta*-PBI.

3.1.3. Thermal properties

The thermal stabilities of both phenylindane-PBI and *meta*-PBI were studied using TGA under nitrogen flow (Fig. 6) and all of the weight loss calculations were based on the dry weight of polymers after water removal. The initial water loss of *meta*-PBI between room temperature and ca. 300 °C was 16.73 wt%, which is consistent with previous results (for reference, the moisture content of *m*-PBI is 15–18 wt% [37]). In contrast, phenylindane-PBI showed much lower moisture content of 5.56 wt%, which was attributed to the hydrophobic characteristic of aliphatic five-member ring within the phenylindane moiety. Decomposition temperatures at different weight losses (0.02 wt%, 5 wt%, and 10 wt%) and weight retained at 900 °C of both PBIs are given in Table 1. The data illustrate that both polymers exhibit excellent thermal stability (less than 5 wt% loss at 500 °C), which is characteristic of the rigid aromatic polymer backbones. The thermal stability of phenylindane-PBI was slightly lower than that of *meta*-PBI due to the introduction of phenylindane linkages into the polymer main chain but it is still sufficient for realistic fuel cell applications.

3.1.4. Density and estimated fractional free volume (FFV)

The densities of phenylindane-PBI and *meta*-PBI were measured using approximately 100 mg pre-dried PBI powders in a gravity bottle at 30 °C. Water was employed as a solvent for initial measurements but the results were found to be unreliable due to the strong water absorption of PBIs as discussed in Section 3.1.3. Therefore, cyclohexane was chosen as a suitable solvent since it is not absorbed by PBIs and has a relatively low density (0.76919 g cm^{-3}, 30 °C). The densities of phenylindane-PBI and *meta*-PBI were found to be 1.16 g cm^{-3} and 1.33 g cm^{-3}, respectively. The *meta*-PBI density measured in this work was similar to previous results (1.3 g cm^{-3} and 1.269 g cm^{-3}) [38,39]. The fractional free volume (FFV) was calculated using Bondi's group contribution approach [40] and the results are shown in Table 1. Phenylindane-PBI exhibited a larger FFV (FFV = 0.162) than *meta*-PBI (FFV = 0.136), indicating a less efficient polymer chain packing which was attributed to the introduction of the rigid bent phenylindane linkages.

3.1.5. Solubility

The solubility characteristics of PBIs shown in Table 2 were evaluated at ambient temperature. Although the dissolution properties of *meta*-PBI have been widely reported, the results are somewhat controversial. The reported dissolution properties of *meta*-PBI have varied due to factors such as preparative methods, polymer molecular weight (IV), and dissolution conditions. Therefore, a *meta*-PBI with IV of 1.39 dL g^{-1} was used in this study for comparison with phenylindane-PBI. Under these conditions, *meta*-PBI was only partially soluble in selected polar aprotic solvents such as DMAc, DMAc/LiCl (4 wt%), and NMP at a relatively low concentration (3.0 wt%). The solubility of phenylindane-PBI was much better than *meta*-PBI and at ambient temperature the polymer was mostly dissolved in these polar aprotic solvents with

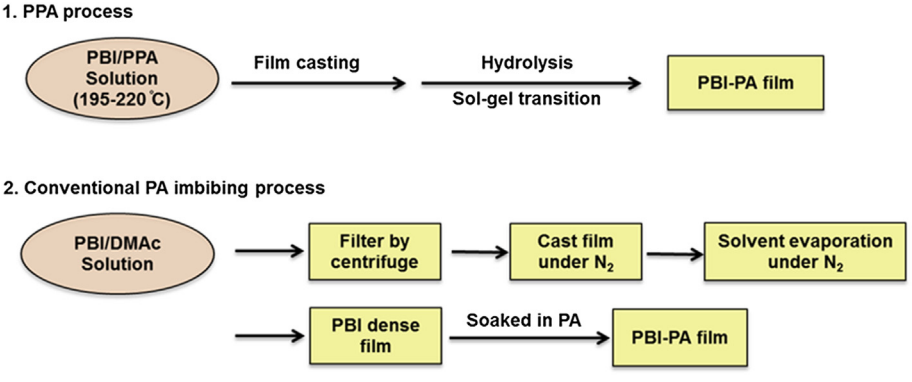

Fig. 7. PA-doped phenylindane-PBI membranes prepared by two different preparation methods (top: PPA process; bottom: conventional PA imbibing process).

concentrations up to 10.0 wt%. These results demonstrated that the introduction of the bulky bent phenylindane structure into the polymer backbone was effective in improving the polymer's solubility. However, both PBIs were insoluble in common organic solvents such as acetone, THF, or methanol.

3.2. Membrane preparation and characterization

3.2.1. Membrane preparation

As shown in Fig. 7, two different processes (PPA process and conventional PA imbibing process) were applied to the preparation of PA-doped phenylindane-PBI membranes. The novel PPA process, developed by Benicewicz et al., offers advantages such as an easier processing procedure and higher membrane acid doping levels as compared to the conventional imbibing process [10,27]. Therefore, our initial work focused on the preparation of acid-doped membranes via the PPA process. However, the PA-doped phenylindane-PBI membranes (Fig. 8(left)) obtained were opaque and mechanically weak, indicating strong phase separation instead of gel formation. The film was not suitable for proton conductivity and fuel cell performance studies. The conventional PA imbibing method was also investigated and the initial films that were cast and dried in the open air were opaque and mechanically weak which was attributed to the strong water absorption and phase separation. In contrast, films obtained in a dry nitrogen environment were transparent and much stronger, as shown in Fig. 8(right). For comparison, PA-doped *meta*-PBI membranes were also prepared by the conventional imbibing process.

3.2.2. Acid absorption

The acid absorption behaviors of PBIs have been studied previously and it was reported that *meta*-PBI could be doped as high as 16 PA/RU although the loss of mechanical integrity was noted at higher doping levels [41,42]. In this work, phenylindane-PBI and *meta*-PBI dense membranes were doped by immersion into PA solutions with different concentrations (70%–90%) for more than 48 h to study and compare their absorption and stability behaviors in PA. As shown in Fig. 9, both phenylindane-PBI and *meta*-PBI showed similar trends of increasing PA doping levels with increasing PA concentrations. The phenylindane-PBI exhibited good stability in 90% PA solution with a doping level of approximately 22 PA/RU but produced a soft membrane. The PA doping levels of phenylindane-PBI in 70%, 80%, and 85% PA solutions were 5.7, 7.3, and 10.0 PA/RU, respectively. For comparison, *meta*-PBI was stable in 85% PA and became partially dissolved in 90% PA after a few hours. The PA doping levels of *meta*-PBI in 70–85% PA solution (3.8–10.3 PA/RU) were slightly lower than those of phenylindane-PBI. However, it is important to note the differences in the formula weight of the different repeat units. Therefore, the phosphoric acid weight percentages (without the water) were also calculated for the two PBIs at different acid doping levels (Fig. 10). For similar acid doping levels, *meta*-PBI membranes possessed a higher acid weight percentage than phenylindane-PBI membranes.

Fig. 8. PA-doped PBI membrane preparation methods.

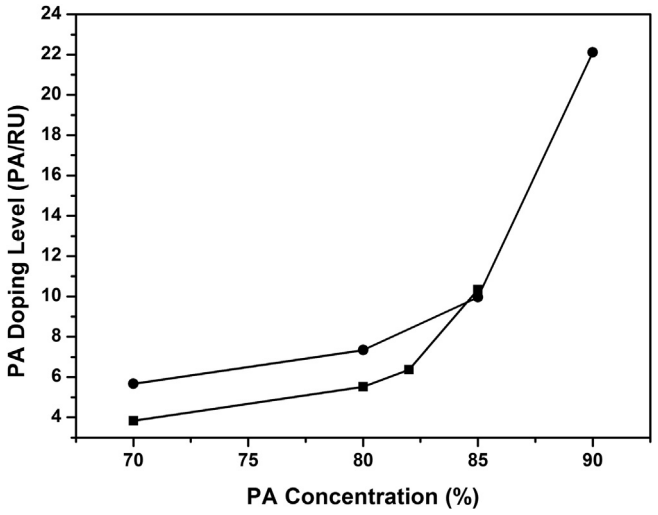

Fig. 9. PA doping level of phenylindane-PBI (circle) and *meta*-PBI (square) treated with different PA concentrations.

3.2.3. Mechanical properties

As noted previously for PA-doped PBI membranes, there is often a tradeoff between acid doping level and mechanical properties [9]. Higher acid doping levels usually provide higher membrane ionic conductivity but can result in drawbacks such as loss of mechanical strength and leaching out of "free" acid during the fuel cell operation [43]. The mechanical properties of phenylindane-PBI (IV = 1.00 dL g^{-1}) and *meta*-PBI with similar IV's (IV = 1.18 dL g^{-1}) were studied as a function of PA doping level at ambient conditions (Figs. 11 and 12). It was found that both the tensile strength and modulus of these membranes were reduced drastically when doped with PA due to the plasticization effect but generally showed similar properties at high doping levels.

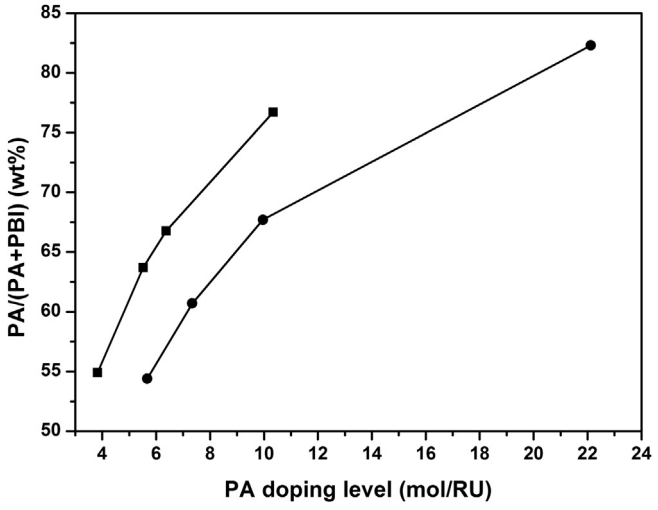

Fig. 10. PA weight percentages of phenylindane-PBI (circle) and *meta*-PBI (square) at different acid doping levels.

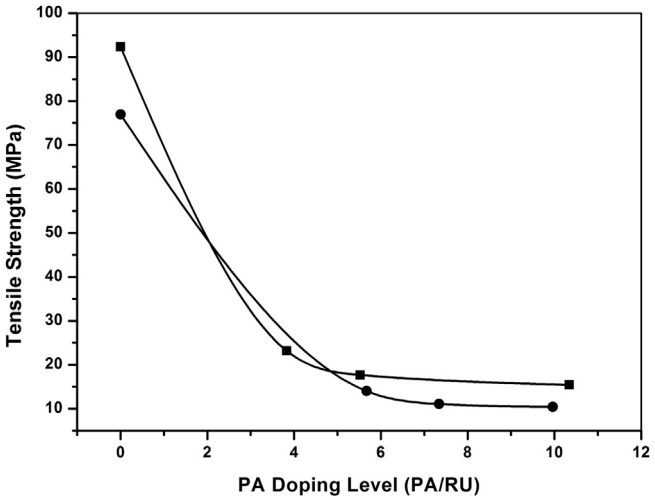

Fig. 11. Tensile strength of PBI membranes (circle: phenylindane-PBI; square: *meta*-PBI) as a function of PA doping level at ambient temperature.

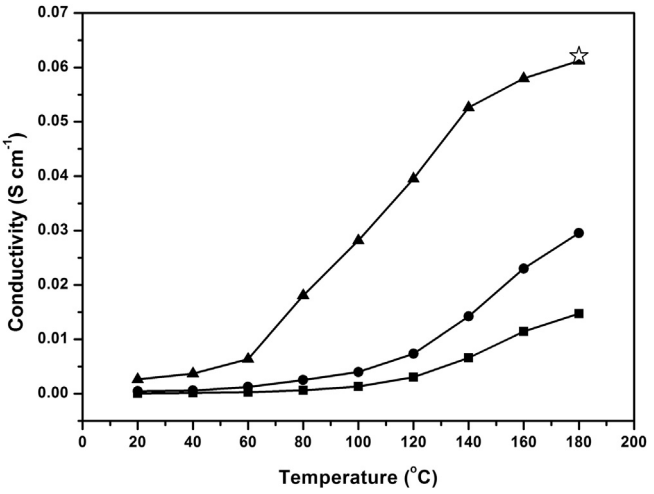

Fig. 13. Proton conductivities of PA-doped phenylindane-PBI membranes (square: 5.7 PA/RU; round: 7.4 PA/RU; triangle: 10.0 PA/RU) and PA-doped *meta*-PBI membranes (unfilled star: 6.4 PA/RU).

3.2.4. Proton conductivity

Proton conductivities of phenylindane-PBI membranes with different acid doping levels were measured from room temperature to 180 °C without humidification and are shown in Fig. 13. As expected, the proton conductivities increased with both temperature and PA doping levels. At relatively low temperatures (<80 °C), the membrane conductivities were all below 0.01 S cm^{-1} and the differences between them were relatively small. As the temperature increased from 80 °C to 180 °C, the conductivities increased and the differences also became larger. For a phenylindane-PBI membrane with a doping level of 10.0 PA/RU, the maximum proton conductivity was 0.061 S cm^{-1} at 180 °C. For comparison, the PA-doped *meta*-PBI membrane showed a similar conductivity of 0.062 S cm^{-1} but with a lower acid loading (6.4 PA/RU). However, when comparisons are made based on the PA weight percentage in the membrane, both membranes contained approximately 67 wt% PA, and exhibited nearly identical proton conductivities.

3.3. Fuel cell testing

Phenylindane-PBI membranes with a PA doping level of 10.0 PA/RU were chosen for the initial MEA fabrications. However, the fuel cell results showed that the membrane mechanical properties were not sufficient for cell operation and pinholes were created during the hot-pressing procedure. As evidence, low open circuit voltages (OCV) (<0.8 V) were observed during the initial fuel cell testing which were attributed to gas cross-over. Therefore, the phenylindane-PBI membrane with a lower PA loading (7.4 PA/RU) and higher mechanical properties was used for subsequent fuel cell studies. The membranes were dipped in 85% PA for a few seconds (10–20 s) prior to MEA fabrication to decrease the interfacial resistance between the membrane and electrodes.

Fuel cell performance studies were conducted on single 10 cm^2 cells. Figs. 14 and 15 show the polarization curves of phenylindane-PBI membranes obtained under H_2/air (**a**) and H_2/O_2 (**b**) (supplied

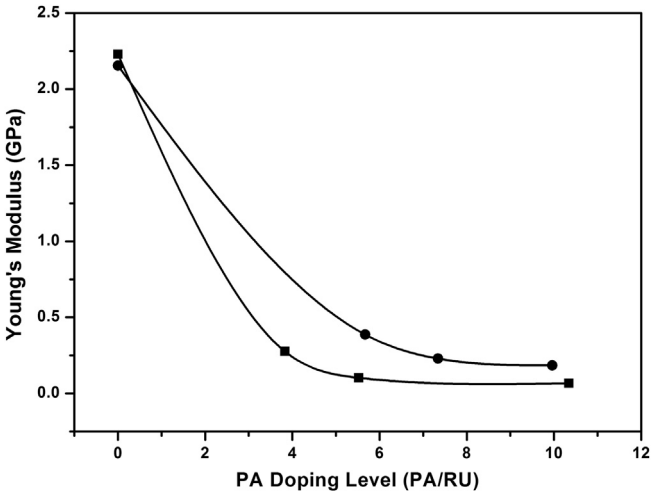

Fig. 12. Young's modulus of PBI membranes (circle: phenylindane-PBI; square: *meta*-PBI) as a function of PA doping level at ambient temperature.

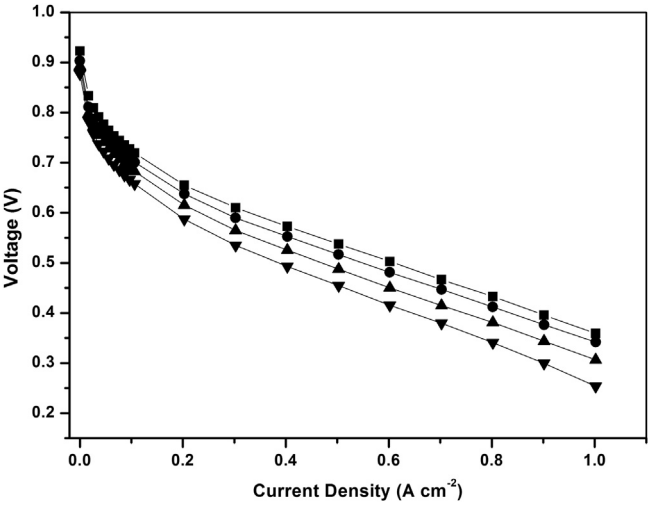

Fig. 14. Polarization curves for MEAs using phenylindane-PBI membrane under H_2/air at various temperatures: squares – 180 °C; circles – 160 °C; uptriangles – 140 °C; downtriangles – 120 °C. (Fuel cell operation conditions: atmospheric pressure (1 atm), constant stoic H_2 (λ = 1.2)/air (λ = 2.0), no external humidification).

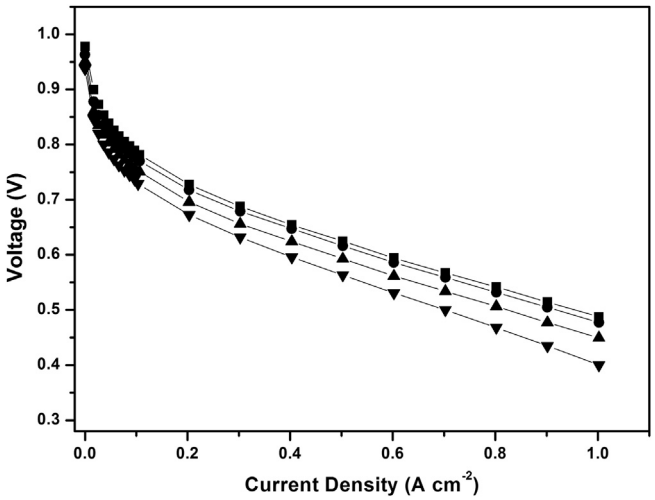

Fig. 15. Polarization curves for MEAs using phenylindane-PBI membrane under H_2/O_2 at various temperatures: squares – 180 °C; circles – 160 °C; uptriangles – 140 °C; downtriangles – 120 °C. (Fuel cell operation conditions: atmospheric pressure (1 atm), constant stoic H_2 (λ = 1.2)/O_2 (λ = 2.0), no external humidification).

at 1.2 and 2.0 stoichiometric flows) over a range of temperatures (120–180 °C). With both oxidants, the fuel cell performance of phenylindane-PBI membranes gradually increased with temperature. At 180 °C and a current density of 0.2 A cm^{-2}, the cell voltage of phenylindane-PBI in H_2/air was approximately 0.66 V and increased to approximately 0.72 V when the gases were switched to H_2/O_2, which was attributed to the increased oxygen partial pressure (from 0.21 atm to 1 atm). For comparison, *meta*-PBI membranes with similar PA doping levels (PA = 7.7 PA/RU) were also tested using the same MEA preparation and fuel cell testing conditions (1 atm), 180 °C, H_2/air (1.2 and 2.0 stoichiometric flows) (Fig. 16). The *meta*-PBI showed similar fuel cell performance at low current densities but a higher rate of voltage loss as the current density was increased into the gas transport loss region when compared with phenylindane-PBI. The maximum power density using H_2/air of phenylindane-PBI was approximately 0.36 W cm^{-2}, which was higher than *meta*-PBI (approximately 0.32 W cm^{-2}).

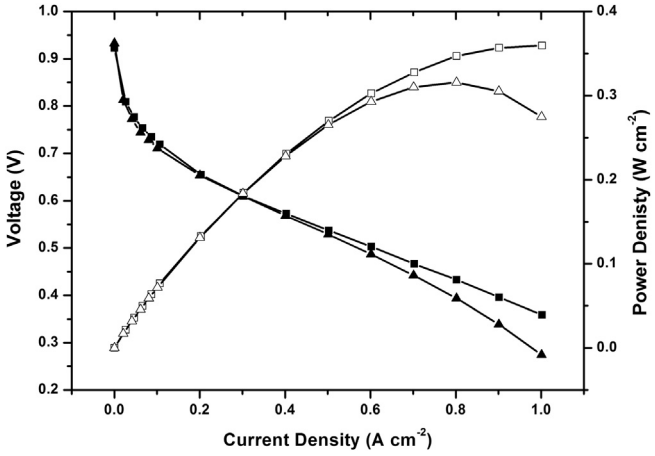

Fig. 16. Polarization curves (filled symbols) and power density curves (unfilled symbols) for MEAs using phenylindane-PBI membranes (squares) and *meta*-PBI membranes (uptriangles). (Fuel cell operation conditions: atmospheric pressure (1 atm), 180 °C, constant stoic H_2 (λ = 1.2)/air (λ = 2.0), no external humidification).

4. Conclusions

A high molecular weight, thermally stable, and organo-soluble phenylindane-PBI was synthesized from 3,3′,4,4′-tetraaminobiphenyl and 1,1,3-trimethyl-3-phenylindan-4′,5-dicarboxylic acid in PPA. Investigation of polymerization conditions to achieve high molecular weight polymers was explored by varying the initial monomer concentrations. A *meta*-PBI with similar IV was also prepared in PPA for detailed comparisons. The TGA curves showed that the thermal stability of phenylindane-PBI was slightly lower than that of *meta*-PBI but still sufficient for practical fuel cell applications. The introduction of the rigid and bent phenylindane moiety into the PBI backbone disrupted the close polymer chain packing, as evidenced by the higher FFV and increased solubility of phenylindane-PBI compared with *meta*-PBI. Acid-doped PBI membranes were prepared by both the PPA process and the conventional imbibing process, and the latter process produced membranes at intermediate doping levels with mechanical properties that could be tested in fuel cells. The relationships among PA concentrations, PA doping levels, and mechanical properties of the phenylindane-PBI membranes and *meta*-PBI membranes were also evaluated and compared. Phenylindane-PBI membranes could be doped to approximately 10.0 PA/RU in 85% PA solution which exhibited a proton conductivity of 0.062 S cm^{-1} at 180 °C. Fuel cells based on the PA-doped phenylindane-PBI membranes showed 0.65 V at 0.2 A cm^{-2} for hydrogen/air at 180 °C when operated at atmosphere pressure and dry gases. The fuel cell performance was slightly higher than the PA-doped *meta*-PBI membrane prepared and tested under similar conditions.

Acknowledgments

The authors gratefully acknowledge the U.S. DOE/EERE-ITP for partial financial support of the project under contract CPS#18990.

References

[1] Q. Li, R. He, J.O. Jensen, N.J. Bjerrum, Chemistry of Materials 15 (2003) 4896–4915.
[2] C. Yang, P. Costamagna, S. Srinivasan, J. Benziger, A.B. Bocarsly, Journal of Power Sources 103 (2001) 1–9.
[3] J. Zhang, Z. Xie, J. Zhang, Y. Tanga, C. Song, T. Navessin, Z. Shi, D. Song, H. Wang, D.P. Wilkinson, Z.-S. Liu, S. Holdcroft, Journal of Power Sources 160 (2006) 872–891.
[4] Y.-L. Ma, J.S. Wainright, M.H. Litt, R.F. Savinell, Journal of The Electrochemical Society 151 (2004) A8–A16.
[5] P. Jannasch, Current Opinion in Colloid & Interface Science 8 (2003) 96–102.
[6] J.S. Wainright, J.-T. Wang, D. Weng, R.F. Savinell, M. Litt, Journal of The Electrochemical Society 142 (1995) L121–L123.
[7] M. Litt, R. Ameri, Y. Wang, R. Savinell, J.S. Wainwright, Materials Research Society Symposium Proceedings 548 (1999) 313–314.
[8] J.S. Wainright, M.H. Litt, R.F. Savinell, in: W. Vielstichm, A. Lamm, H.A. Gasteiger (Eds.), Handbook of Fuel Cells, John Wiley & Sons Ltd., New York, 2003, pp. 436–446.
[9] Q. Li, J.O. Jensen, R.F. Savinell, N.J. Bjerrum, Progress in Polymer Science 34 (2009) 449–477.
[10] L. Xiao, H. Zhang, E. Scanlon, L.S. Ramanathan, E.-W. Choe, D. Rogers, T. Apple, B.C. Benicewicz, Chemistry of Materials 17 (2005) 5328–5333.
[11] Q. Li, C. Pan, J.O. Jensen, P. Noye, N.J. Bjerrum, Chemistry of Materials 19 (2007) 350–352.
[12] Y. Zhai, H. Zhang, Y. Zhang, D. Xing, Journal of Power Sources 169 (2007) 259–264.
[13] P. Noyé, Q. Li, C. Pan, N.J. Bjerrum, Polymers for Advanced Technologies 19 (2008) 1270–1275.
[14] N. Xu, X. Guo, J. Fang, H. Xu, J. Yin, Journal of Polymer Chemistry Part A: Polymer Chemistry 47 (2009) 6992–7002.
[15] M. Hazarika, T. Jana, ACS Applied Materials & Interfaces 4 (2012) 5256–5265.
[16] D. Arunbabu, A. Sannigrahi, T. Jana, The Journal of Physical Chemistry B 112 (2008) 5305–5310.
[17] V. Deimede, G.A. Voyiatzis, J.K. Kallitsis, Q. Li, N.J. Bjerrum, Macromolecules 33 (2000) 7609–7617.
[18] Q. Li, H.C. Rudbeck, A. Chromik, J.O. Jensen, C. Pan, T. Steenberg, M. Calverley, N.J. Bjerrum, J. Kerres, Journal of Membrane Science 347 (2010) 260–270.
[19] R.H. He, Q. Li, G. Xiao, N.J. Bjerrum, Journal of Membrane Science 226 (2003) 169–184.

[20] P. Staiti, M. Minutoli, S. Hocevar, Journal of Power Sources 90 (2000) 231–235.
[21] S.-W. Chuang, S.L.-C. Hsu, Journal of Polymer Chemistry Part A: Polymer Chemistry 44 (2006) 4508–4513.
[22] H. Pu, L. Wang, H. Pan, D. Wan, Journal of Polymer Chemistry Part A: Polymer Chemistry 48 (2010) 2115–2122.
[23] J. Yang, Q. Li, L.N. Cleemann, C. Xu, J.O. Jensen, C. Pan, N.J. Bjerrum, R. He, Journal of Materials Chemistry 22 (2012) 11185–11195.
[24] T.H. Kim, S.K. Kim, T.W. Lim, J.C. Lee, Journal of Membrane Science 323 (2008) 362–370.
[25] S. Yu, B.C. Benicewicz, Macromolecules 42 (2009) 8640–8648.
[26] A.L. Gulledge, B. Gu, B.C. Benicewicz, Journal of Polymer Chemistry Part A: Polymer Chemistry 50 (2012) 306–313.
[27] S. Yu, L. Xiao, B.C. Benicewicz, Fuel Cells 8 (2008) 165–174.
[28] G. Qian, D.W. Smith Jr., B.C. Benicewicz, Polymer 50 (2009) 3911–3916.
[29] R.S. Bhavsar, S.B. Nahire, M.S. Kale, S.G. Patil, P.P. Aher, R.A. Bhavsar, U.K. Kharul, Journal of Applied Polymer Science 120 (2011) 1090–1099.
[30] Y. Ding, B. Bikson, Polymer 43 (2002) 4709–4714.
[31] G. Maier, M. Wolf, M. Bleha, Z. Pientka, Journal of Membrane Science 143 (1998) 105–113.
[32] G. Maier, M. Wolf, M. Bleha, Z. Pientka, Journal of Membrane Science 143 (1998) 115–123.
[33] H. Zhang, Novel Phosphoric Acid Doped Polybenzimidazole Membranes for Fuel Cells. Ph.D. thesis, Rensselaer Polytechnic Institute, 2004.
[34] B.C. Ward, US Patent, 4588808, 1986.
[35] B.C. Ward, US Patent, 4672104, 1987.
[36] B.G. Dawkins, J.D. Baker, R.H. Joiner, US Patent, 7060782, 2006.
[37] A.S. Buckley, D.E. Stuetz, G.A. Serad, Encyclopedia of Polymer Science and Engineering 11 (1987) 572–601.
[38] E. Foldes, E. Fekete, F.E. Karasz, B. Pukanszky, Polymer 41 (2000) 975–983.
[39] M.R. Tarasevich, Z.R. Karichev, V.A. Bogdanovskaya, L.N. Kuznetsova, B.N. Efremov, A.V. Kapustin, Russian Journal of Electrochemistry 40 (2004) 653–656.
[40] A. Bondi, The Journal of Physical Chemistry 68 (1964) 441–451.
[41] Q. Li, R. He, J.O. Jensen, N.J. Bjerrum, Fuel Cells 4 (2004) 147–159.
[42] Q. Li, H.A. Hjuler, N.J. Bjerrum, Journal of Applied Electrochemistry 31 (2001) 773–779.
[43] J.W. Lee, S.B. Khan, K. Akhtar, K.I. Kim, Tae-Won Yoo, K.W. Seo, H. Han, A.M. Asiri, International Journal of Electrochemical Science 7 (2012) 6276–6288.